Adhesion properties of regenerated lignocellulosic fibres towards poly(lactic acid) microspheres assessed by colloidal probe technique

(article starts on next page)

Regular Article

Adhesion properties of regenerated lignocellulosic fibres towards poly (lactic acid) microspheres assessed by colloidal probe technique

Jérôme Colson [a], Torbjörn Pettersson [b], Shirin Asaadi [c], Herbert Sixta [c], Tiina Nypelö [d], Andreas Mautner [e], Johannes Konnerth [a],*

[a] University of Natural Resources and Life Sciences Vienna, Department of Materials Sciences and Process Engineering, Institute of Wood Technology and Renewable Materials, Konrad-Lorenz-Straße 24, 3430 Tulln, Austria
[b] KTH Royal Institute of Technology, Department of Fibre and Polymer Technology, Division of Fibre Technology, Teknikringen 58, 100 44 Stockholm, Sweden
[c] Aalto University, School of Chemical Engineering, Department of Bioproducts and Biosystems, Vuorimiehentie 1, 02150 Espoo, Finland
[d] Chalmers University of Technology, Department of Chemistry and Chemical Technology, Kemigården 4, 412 96 Göteborg, Sweden
[e] University of Vienna, Faculty of Chemistry, Institute of Materials Chemistry & Research, Währinger Straße 42, 1090 Vienna, Austria

GRAPHICAL ABSTRACT
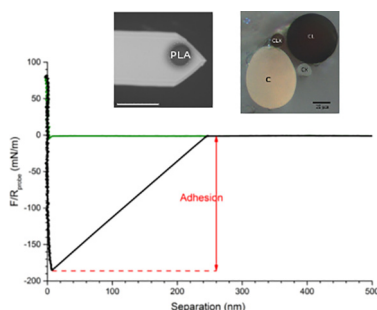
ARTICLE INFO

ABSTRACT

In the field of polymer reinforcement, it is important to understand the interactions involved between the polymer matrix and the reinforcing component. This paper is a contribution to the fundamental understanding of the adhesion mechanisms involved in natural fibre reinforced composites. We report on the use of the colloidal probe technique for the assessment of the adhesion behaviour between poly(lactic acid) microspheres and embedded cross-sections of regenerated lignocellulosic fibres. These fibres consisted of tailored mixtures of cellulose, lignin and xylan, the amount of which was determined beforehand. The influence of the chemical composition of the fibres on the adhesion behaviour was studied in ambient air and in dry atmosphere. In ambient air, capillary forces resulted in larger adhesion between the sphere and the fibres. Changing the ambient medium to a dry nitrogen atmosphere allowed reducing the capillary forces, leading to a drop in the adhesion forces. Differences between fibres of distinct chemical compositions could be measured only on freshly cut surfaces. Moreover, the surface energy of the fibres was assessed by inverse gas chromatography. Compared to fibres containing solely cellulose, the presence of lignin and/or hemicellulose led to higher adhesion and lower surface energy, suggesting that these chemicals could serve as natural coupling agents between hydrophobic and hydrophilic components.

* Corresponding author.
E-mail addresses: jerome.colson@boku.ac.at (J. Colson), torbj@kth.se (T. Pettersson), shirin.asaadi@aalto.fi (S. Asaadi), herbert.sixta@aalto.fi (H. Sixta), tiina.nypelo@chalmers.se (T. Nypelö), andreas.mautner@univie.ac.at (A. Mautner), johannes.konnerth@boku.ac.at (J. Konnerth).

1. Introduction

Composite materials can be found in a wide range of technical applications. These materials are tailored for specific load cases by combining the properties of individual components. For example, the combination of compression resistant concrete with tension resistant steel frames has become a standard material in the construction industry. In the past decades, interest in natural fibre reinforced composites has dramatically increased. Indeed, natural fibres showing high specific mechanical properties in relation to their low density are available in high amount and at low cost in nature. Moreover, their production is much more energy-efficient than for glass fibres, which require high temperatures and therefore a high energy input. This makes natural fibre-reinforced composites ideal candidates in the search for bio-based, sustainable materials [1].

One of the major causes of failure for natural fibre reinforced composites is insufficient compatibility between the polymer matrix and the reinforcing fibres, the former being hydrophobic and the latter hydrophilic in most of the cases – coupling agents such as maleic anhydride are often used to overcome this issue [2]. Due to the inherent incompatibility between the phases, it is important to characterize the interface of the obtained composites. This can be done in various ways. On a large scale, mechanical testing (e.g. tensile tests) is the method of choice: with appropriate equipment, it quickly and easily provides data about strength and stiffness of a composite material. However, this method needs the tested materials to be run through the entire manufacturing process. Moreover, the results relate not only to the fibre/matrix adhesion, but also to other parameters such as fibre length distribution, roughness, orientation and homogeneity of the fibre dispersion in the matrix [3].

From a fundamental point of view, it is necessary to understand the mechanisms involved in fibre/matrix adhesion at the micro- to nanometre scale. This is particularly true when natural lignocellulosic fibres are intended to be used for reinforcement purposes, as the influence of every single component is still not fully understood. Some authors highlighted the fact that lignin, because of the presence of both hydrophobic and hydrophilic functional groups, could act as a natural coupling agent between the rather non-polar polymer matrix and the polar fibres [4,5]. Similarly to lignin, hemicelluloses such as xylan have been discussed to provide superior compatibility between highly polar cellulose-based fibres (e.g. micro or nanofibrillated cellulose) and non-polar polymeric matrices [6]. However, a drawback of natural lignocellulosic fibres is their intrinsic chemical heterogeneity. Analyses with well-defined model compounds such as regenerated lignocellulosic fibres can help to overcome this limitation and improve our knowledge of the interactions involved in natural fibre reinforced polymers.

Different adhesion mechanisms come into play in a composite material and factors such as mechanical interlocking, chemical bonding, inter diffusion and interfacial energy are important for the final properties of the composite. The latter three factors are difficult to determine in a readymade composite, but they determine the dispersibility of the fibrous material in the matrix. One way to understand the influence of these factors is to study the interactions between the fibres and the matrix on a micrometre or nanometre scale. On these smaller length scales, measurement of surface interaction can help to understand the compatibility between two materials, through the assessment of the adhesion (i.e. the force needed to separate the two different surfaces from each other). Surface interactions and adhesion can be measured with, for example, atomic force microscope (AFM) [7,8], surface force apparatus [9] or Johnson-Kendall-Roberts (JKR) apparatus

[10]. Among the AFM-based techniques, colloidal probe technique [11,12] has proven useful in a wide variety of fields over the years, both in fundamental and applied research [13]. The core of the method is the use of an AFM cantilever as a force sensor onto which a micrometre sized particle is attached. When smooth, micrometre-sized spheres are glued at the end of the cantilever, interactions at interfaces of asymmetric systems as rationalised in Derjaguin-Landau-Evert-Verwey-Overbeek (DLVO) theory [14,15] can be measured.

This technique has already been used in the field of natural fibres. For example, Holmberg et al. and Radtchenko et al. studied the adhesion between flat cellulose surfaces and silica microbeads [16,17]. Closer to applied research in natural fibre composites, other research groups assessed the surface forces between nanometre smooth cellulose spheres [18], or studied the behaviour of such spheres with regard to polymers [19] or wood components such as lignin [20]. Polymer microspheres have also already been used and their adhesion towards flat cellulose films prepared by spin-coating [21] or Layer-by-Layer (LbL) deposition [22] has been studied. However, the influence of individual compounds, such as hemicelluloses or lignin commonly being present in natural fibres, has not been investigated so far.

In this paper, we assess the influence of the chemical composition of regenerated lignocellulosic fibres (containing cellulose, hemicellulose and lignin in given proportions which thus impacting the surface polarity) on their adhesion towards poly(lactic acid) (PLA) microspheres. PLA is one of the most promising polymers in the field of natural fibres reinforced composites, and that is why it is important to understand its interactions with lignocellulosic fibres. Moreover, the adhesion behaviour of the fibres is put into relation with their surface energy.

2. Materials and methods

2.1. Materials

Ultrapure water (18.2 MΩ cm) was obtained from a Milli-Q® IQ 7000 water purification system (Merck Millipore, Billerica, MA, USA). Dichloromethane CH_2Cl_2 was obtained from Merck Millipore (Billerica, MA, USA). Polyvinyl alcohol (Mowiol® 4–88, M_w = 31,000 g/mol) was purchased from Sigma-Aldrich (St. Louis, MI, USA). Poly(lactic acid) (Ingeo 3052D) was obtained from NatureWorks (Minnetonka, MN, USA).

Hexane, heptane, octane, nonane, decane, dichloromethane, acetone, acetonitrile and ethyl acetate for inverse gas chromatography were purchased in HPLC-grade from Sigma-Aldrich.

2.2. Fibre preparation

Regenerated fibres containing different amounts of cellulose, lignin and hemicellulose (xylan) were prepared using the Ioncell-F process, as described in detail elsewhere [23]. Low draw ratios of 0.5–0.6 were used to obtain fibre diameters up to 60 μm and facilitate the positioning of the microspheres on the fibre cross sections in the measurements described below. Four different fibre types were used: Cellulose (C), Cellulose/Lignin (CL), Cellulose/Lignin/Xylan (CLX) and Cellulose/Xylan (CX). Determination of the fibre composition was performed according to NREL standard/TP-510-42618 [24]. The results are presented in Table 1.

The fibres were embedded into PLA. For this purpose, PLA was molten at 250 °C and cast into a mould containing aligned fibres. Small blocks (approximately 3 mm high, 2 mm wide and 3 mm long) were cut with a razor blade and glued on a metal disk, the

Table 1
Chemical composition of the samples and diameters of the fibres selected for force measurements.

Sample	Cellulose content (%)	Lignin content (%)	Xylan content (%)	Draw ratio	Diameter (μm)		
					Fibre 1	Fibre 2	Fibre 3
C	94.24	0.00	5.52	0.5	48.6	56.4	54.9
CX	78.19	2.25	19.56	0.6	38.9	36.1	35.3
CL	71.33	24.31	4.35	0.5	62.1	64.5	60.2
CLX	52.75	22.91	23.66	0.6	42.0	40.8	44.7

fibre cross sections pointing upwards. Smooth cross sections were then produced by successively cutting the sample with several diamond blades (Diatome, Nidau, Switzerland) in an ultramicrotome (Ultracut-R, Leica, Wetzlar, Germany). The blades, cutting speeds and cutting thicknesses were the following: Ultratrim (up to 30 mm/s, 400 nm), Histo (1 mm/s, 400 nm, 200 nm and 100 nm) and finally Ultra-AFM (1 mm/s, 100 nm, 50 nm and 20 nm). Four PLA blocks each containing a different fibre type (C, CL, CLX or CX) and one additional block containing one fibre of each type were prepared in this way. Accumulation of electrostatic charges on the sample surface was avoided by using an antistatic gun (Zerostat 3, Milty, Hertfordshire, United Kingdom) after the last cutting step.

The adhesion measurements (as described further in Section 2.5.1 Adhesion measurements) were performed immediately after cutting the samples ("fresh surfaces") as well as after having stored the samples in ambient air for 3 weeks ("aged surfaces"). To avoid biases, storage time was kept constant for all samples prior to measurements, and the measurement conditions were also kept constant.

2.3. Microsphere preparation

PLA microspheres were prepared by a solvent evaporation technique originating from the pharmaceutical field [25]. The production of PLA microspheres intended for colloidal probe measurement has already been described elsewhere [21], and we used the same procedure: PLA was dissolved in CH_2Cl_2 and poured in a PVA/water solution. The resulting solution was stirred overnight at 60 °C. It was finally filtered (Grade 589/3, Whatman, Little Chalfont, Great Britain), the PLA microspheres remaining on the filter were collected and stored in ultrapure water as a 0.005–0.01 wt % suspension.

2.4. Preparation of the colloidal probes

First, widths and lengths of the cantilevers to be used (HQ: CSC37/tipless/No Al and HQ:NSC35/tipless/No Al, MikroMasch, Wetzlar, Germany) were measured under a reflectance optical microscope (Nikon). The resonant frequency and quality factor of each cantilever were determined with the AFM TuneIT software (Järna, Sweden) in a MultiMode IIIa AFM (Veeco Instruments, Santa Barbara, CA, USA). All these parameters were used for hydrodynamic spring constant calibration [26].

A few drops of microsphere suspension (0.005–0.01 wt%) were taken with a glass capillary, deposited onto a microscope slide and air-dried. Due to the low concentration of the suspensions, microsphere agglomeration during drying was avoided. Two component epoxy glue (Power Epoxy Universal Extra Time, Loctite, curing time approximately 4 h) and the chip were deposited on other microscope slides. The slides were then placed under the optical microscope equipped with long working distance lenses. Then, a drop of glue was picked up with an etched tungsten wire and deposited at the very end of the desired, previously calibrated cantilever. Another tungsten wire was used to pick up one microsphere and to deposit it on the glue spot. A micromanipulator (HS 6 Manuell, Märzhäuser Wetzlar GmbH & Co KG, Wetzlar, Germany) was used to achieve the precision required during these steps. Care was taken to select microspheres having similar diameters (compare Table 2). The probe (cantilever with glued microsphere) was then stored in a cantilever box until use (less than one week).

2.5. AFM measurements

2.5.1. Adhesion measurements

One sample, containing all four fibre types embedded in PLA, was scanned with a Dimension Icon scanning probe microscope (Bruker AXS, Santa Barbara, CA, USA) operated in PeakForce quantitative nanomechanical mapping (PF-QNM) mode with a Scanasyst-Air cantilever (Bruker, USA), calibrated according to the operation manual.

For colloidal probe technique, force measurements were performed with a MultiMode IIIa with a Picoforce extension (Veeco Instruments, Santa Barbara, CA, USA). The cantilever with the glued microsphere was placed over the centre of the fibre cross-section. One hundred individual force curves each composed of 10,000 measurement points were captured by rastering the cantilever over the fibre in a 10 × 10 grid, the x/y space between each point being 200 nm. The ramp size was set to 3 μm, using a rate of 2 μm/s, a trigger threshold of 50 nm and a surface delay of 500 ms. These measurements were performed in ambient air (50% relative humidity) and under dry condition (by directing a N_2 flux through the cantilever chamber). A humidity sensor (HumidiPRO, Honeywell, Morristown, NJ, USA) was used to track any accidental variations in humidity and to make sure the humidity in the N_2 saturated atmosphere was recorded as 0%. The temperature was kept constant at 25 °C. The characteristics of the

Table 2
Properties of the cantilevers used on the samples in the different atmospheres. Three cantilevers were used in total. Mean values and standard deviations of the deflection sensitivity were calculated by grouping all individual deflection sensitivities calculated on each sample in a particular atmosphere.

Atmosphere	Sample surface	Cantilever	Spring constant (N/m)	Deflection sensitivity (nm/V)	Microsphere diameter (μm)
Air	fresh	1	5.92	76.3 ± 7.9	15.3
	old	2	6.56	41.7 ± 1.4	16.9
N_2	fresh	1	5.92	75.6 ± 4.6	15.3
	old	3	0.66	100.2 ± 5.3	16.9

cantilevers and microspheres used for these measurements in each setting can be found in Table 2.

Typical force measurement data is shown in Fig. 1a. Care was taken to use cantilevers stiff enough for the deflection to stay within the linear range in the photodiode during the adhesion measurements [27]. Table 2 summarizes the properties of the cantilevers used for the force measurements: On aged surfaces in N_2, the adhesion was expected to be the lowest – a less stiff cantilever was therefore selected accordingly. On the contrary, when the adhesion was expected to be higher (in air because of capillary interactions involved and on the freshly cut surface in N_2, as discussed more extensively in the appropriate sections further on), rather stiff cantilevers were used. Unprocessed raw data from the AFM was converted to force curves (i.e. force vs separation data) using the algorithm described in [28] and the adhesion values were extracted with the AFM ForceIT v3 software (Järna, Sweden). The

adhesion was extracted as the pull-off force (Fig. 1b) – it was calculated from the difference between the zero-load status (baseline value) and the minimum force measured during the retraction movement of the cantilever, as displayed in Eq. (1):

$$F_{adh} = \frac{F_{pull-off}}{R_{probe}} = \frac{k\alpha U}{R_{probe}} \tag{1}$$

were F_{adh} is the normalised adhesion, $F_{pull-off}$ is the pull-off force, R_{probe} is the microsphere radius, k is the cantilever spring constant in, α is the deflection sensitivity and U is the deflection voltage on the photodiode. Deflection sensitivity was calculated directly from the recorded force data in each measurement. It was extracted from the slope of the part marked in green in Fig. 1a, whose linearity indicates that the deformation of the microsphere and the fibre was negligible (hard wall system).
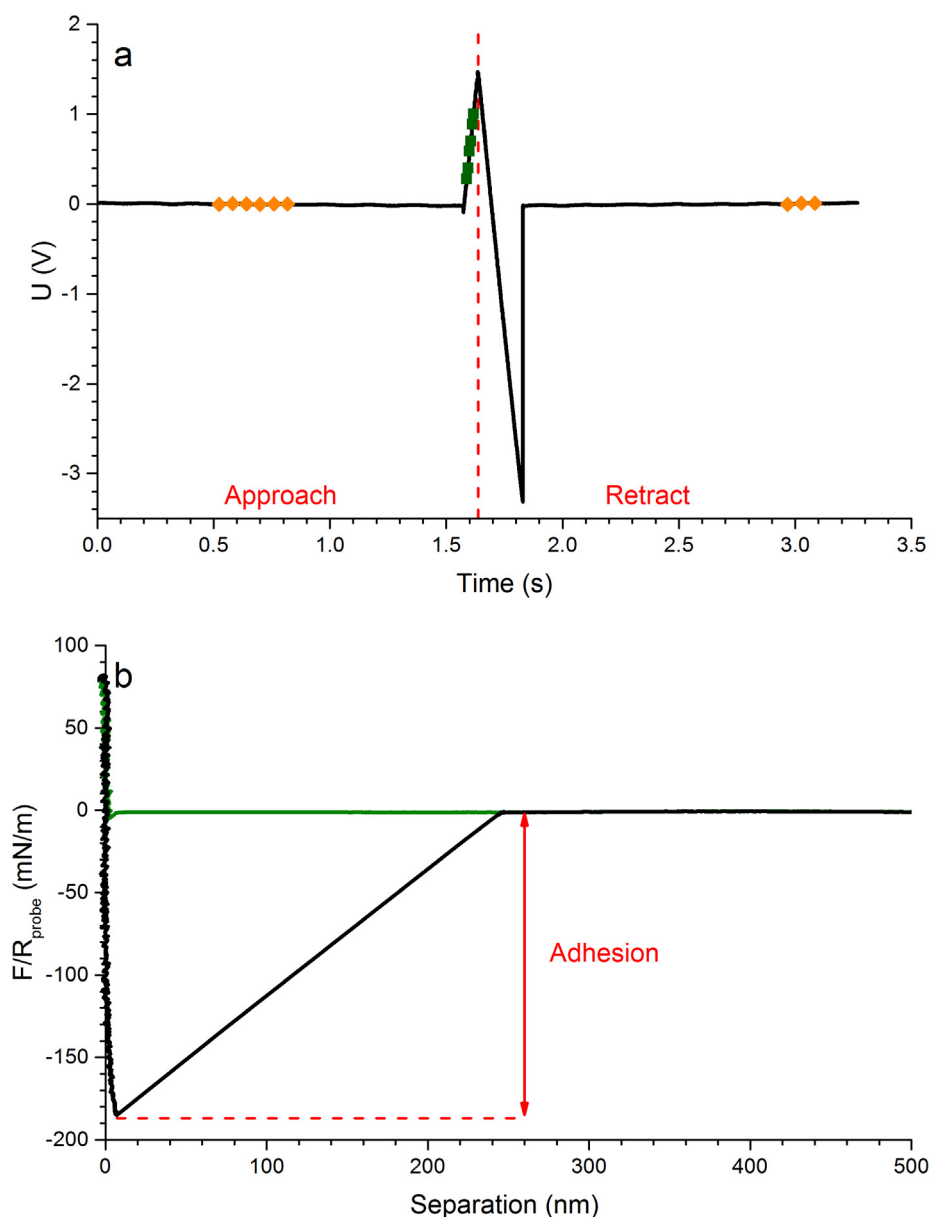

Fig. 1. (a) Typical force measurement data, cantilever deflection (U) vs time. The parts marked in orange were used to calculate the zero load baseline, the part in green was used for the calculation of deflection sensitivity. (b) Typical force curve (normalised force vs separation), green curve on approach and black curve on separation, also indicating the adhesion. (For interpretation of the references to colour in this figure legend, the reader is referred to the web version of this article.)

Mean values and standard deviations of the deflection sensitivities obtained for each cantilever in the different atmospheres are listed in Table 2.

2.5.2. Topography

Besides assessing force curves, the surface topography of the microspheres was checked with a MultiMode 8 AFM (Bruker, Billerica, MA, USA). For this purpose, microspheres on a microscope slide were scanned with a Scanasyst-Air cantilever (f_{nom} = 70 kHz, k_{nom} = 0.4 N/m) in the Bruker Scanasyst mode. The tip velocity was set to 2.5 μm/s. Evaluation of the obtained height maps was done with the Gwyddion 2.49 freeware (www.gwyddion.net). The spherical shape was removed by aligning rows using the built-in polynomial method with the polynomial degree set to 3.

2.6. SEM imaging

The microspheres glued on the cantilevers were imaged with a table-top SEM (TM1000, Hitachi, Chiyoda, Japan). This was done after completion of all colloidal probe measurements with the AFM, as the electron beam was noticed to damage the surface of the microsphere, thereby impacting their roughness.

2.7. Inverse gas chromatography (IGC)

From inverse gas chromatography (IGC; Surface Energy Analyzer, Surface Measurements Systems Ltd., U.K.), the surface energy of the 4 available fibre types (C, CL, CLX, CX) and of the PLA microspheres was established at 30 °C for 0% RH. Samples of the fibres (250–300 mg) were packed into glass columns (inner diameter 3 mm, outer diameter 6 mm), which were plugged with glass wool. A series of alkanes (hexane, heptane, octane, nonane, decane) as well as polar probes dichloromethane, acetone, acetonitrile and ethyl acetate were flown (10 ml/min) over the membrane samples. The retention times and coverages were recorded using a flame ionization detector (FID). From these retention times, the dispersive, specific and total surface energies were computed for a range of sample surface coverages (between 0.001 and 0.2) using the Dorris and Gray method from the peak maximum. The data presented in this paper were obtained at a coverage of 0.001.

3. Results and discussion

3.1. Roughness of the PLA microspheres

As the DLVO theory is valid for flat surfaces, the sample cross-sections and the microspheres used in this paper have to be as close as possible to ideal flat surfaces. The sample cutting method described in the previous section guarantees low root-mean-squared roughness (R_q) around 2 nm for all fibre cross-sections. SEM imaging (Fig. 2a) shows that the surface of the microsphere can be considered to be very smooth. This qualitative observation is quantitatively confirmed by topographic AFM analysis, as shown in Fig. 2b. The overall R_q of the 5 μm × 5 μm recorded height map
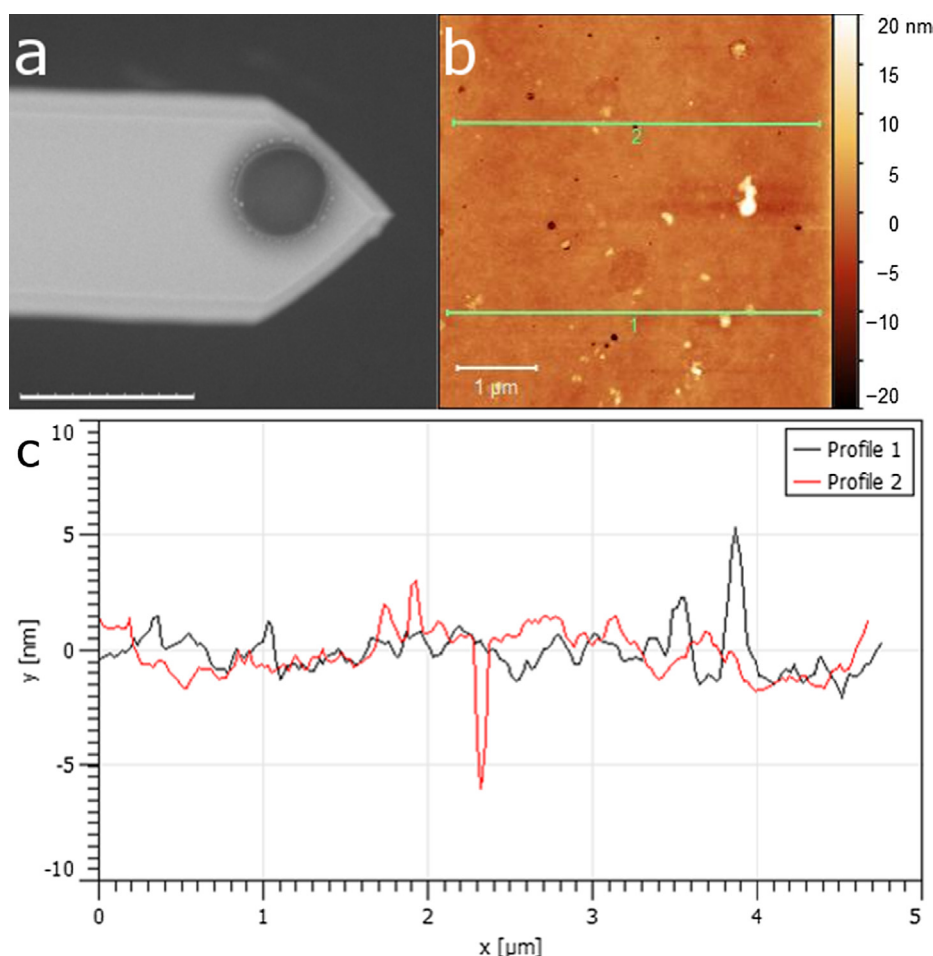

Fig. 2. (a) SEM picture of a PLA sphere glued on a cantilever (scale bar: 30 μm), (b) topography imaging on such a sphere and (c) height profiles as indicated by the green lines in (b). (For interpretation of the references to colour in this figure legend, the reader is referred to the web version of this article.)

was calculated to be 1.7 nm. This value is in accordance with other publications using the same method for the production of the microspheres [21]. On the profiles shown in Fig. 2c, only small variations can be seen, with occasional peaks not exceeding 10 nm in height. With this low roughness, we can conclude that the produced PLA microspheres are suitable for measurements with colloidal probe technique.

3.2. Fibre morphology

Fig. 3a shows the four fibre types as seen in an optical microscope in reflection mode. Differentiation of the fibre types in a cross section demanded light microscopy analysis. In this particular sample, fibres with high draw ratio were selected for cellulose (C) and cellulose/lignin (CL), while low draw ratios were taken for cellulose/xylan (CX) and cellulose/lignin/xylan (CLX). This allowed identification of the four fibre types based on their colour (dark = contains lignin) and diameter. When scanned in the AFM, regenerated fibre types used in this study show differences in adhesion with regard to a standard silicon tip (Fig. 3b and c). In a previous paper, we have shown that distinction between differently polar surfaces is possible in the PeakForce PF-QNM mode when assessing the adhesion signal with such a tip [29]. This can be applied to the identification of differently polar polysaccharides, e.g. in films [30]. In the present case, the four fibre types can clearly be distinguished when a freshly cut surface is scanned (Fig. 3b). CX has the highest adhesion towards a standard silicon tip, followed by C. The lignin-containing fibres show the lowest PF-QNM adhesion values. On an aged surface (Fig. 3c), all fibres show approximately the same adhesion towards a standard silicon tip. Moreover, the adhesion value is lower than on the freshly cut surface, suggesting a decrease in surface polarity with time, as it has recently been observed on wood samples [31].

The uniform colour of the cross section in Fig. 3b and c shows that the adhesion values found on one particular fibre are homogenous. This implies that the polymers are homogeneously distributed over the major part of fibre cross-section. Enrichment in lignin [32] and xylan [33] – which have been shown to occur on the outermost layer of Lyocell type regenerated fibres – would in our case translate in a colour gradient on the fibre cross section in the output data but could not be observed here. This is presumably due to the influence of topography in the transition zone between the fibre and the embedding medium.

3.3. Colloidal probe adhesion measurements

Fig. 4 summarizes the adhesion (i.e. the pull-off force normalized by the probe radius, $F_{pull-off}/R_{probe}$) obtained on all samples in

the different atmospheres. First of all, as shown in Fig. 4b and d, the adhesion amounts to approximately 40 mN/m in air and 20 mN/m in N_2 for all aged samples. No significant differences in the adhesion of the various samples could be found on aged surfaces. Once again, this confirms the loss of surface polarity occurring on lignocellulosic surfaces over time, as it has already been demonstrated on bulk wood [31] as well as on coated wood [34]. In bulk wood, the loss of adhesion after ageing has been hypothesised to be caused by migration of extractives to the surface. However, the correlation between adhesion and extractive content of the surface is rather poor [35,36]. No extractives are present in regenerated fibres, suggesting that other mechanisms (e.g. surface oxidation and/or contamination during storage) are involved. What is more, it has been suggested that the degree of polymerization of the cellulose molecules decreases upon ageing [37], which could also impact the adhesion.

When comparing the measurements done on aged samples in ambient air (Fig. 4b) with those on the same samples in dry atmosphere (Fig. 4d), it is clear that the overall values of the adhesion are about 50% lower in dry atmosphere for each sample type. A humidity level of about 50% in ambient air is sufficient for the creation of a thin layer of condensed water molecules on the surface of the colloid, thereby causing an increase in the measured adhesion [38] attributed to capillary interactions. Other research groups already showed the biasing influence of humidity on adhesion measurements [38,39]. On the fresh samples (Fig. 4a and c), the difference between the obtained values in air and in N_2 is less pronounced, suggesting that the contribution of the adhesion caused by capillary interactions is lower.

On freshly cut surfaces, the 3 fibres tested for each type behave overall similarly. A noticeable exception is the clearly lower adhesion value found for one of the CL type fibres when it is freshly cut. As this is occurring on the same fibre in air and N_2, this behaviour is most probably caused by impurities on the fibre surface. However, apart from this exception, the fibres containing only cellulose (C) show lower adhesion towards the PLA microsphere than the three other fibre types (CL, CLX and CX) on fresh surfaces (Fig. 4 a and c). The measured pull-off force value for pure cellulose is comparable to previously reported cellulose/PLA measurements even though the experimental setup was inverted (cellulose probe on PLA surface) compared to the one used in the present study [40].

The adhesion measured on CL, CLX and CX are of the same order of magnitude (around 150 mN/m in both air and N_2). This suggests that both xylan and lignin have higher affinity towards PLA than pure cellulose. Indeed, the adhesion amounts to only 50–100 mN/m on C. Moreover, Table 1 shows that CX fibres still contain a low amount of lignin (2.25%) which is also expected to
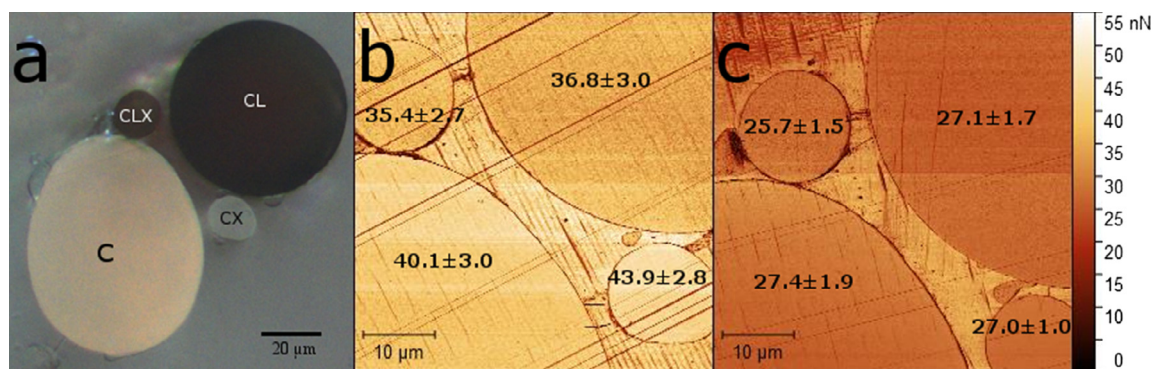

Fig. 3. Optical microscopy (a) and AFM PF-QNM adhesion scan on a fresh (b) and an aged (c) sample of the cellulose, cellulose/xylan, cellulose/lignin and cellulose/xylan/lignin fibres embedded in PLA. The values represent the mean adhesion values and standard deviations obtained on each fibre in nN. For further information concerning the area evaluated on each fibre, please refer to supplementary information S1 displaying the evaluation masks.
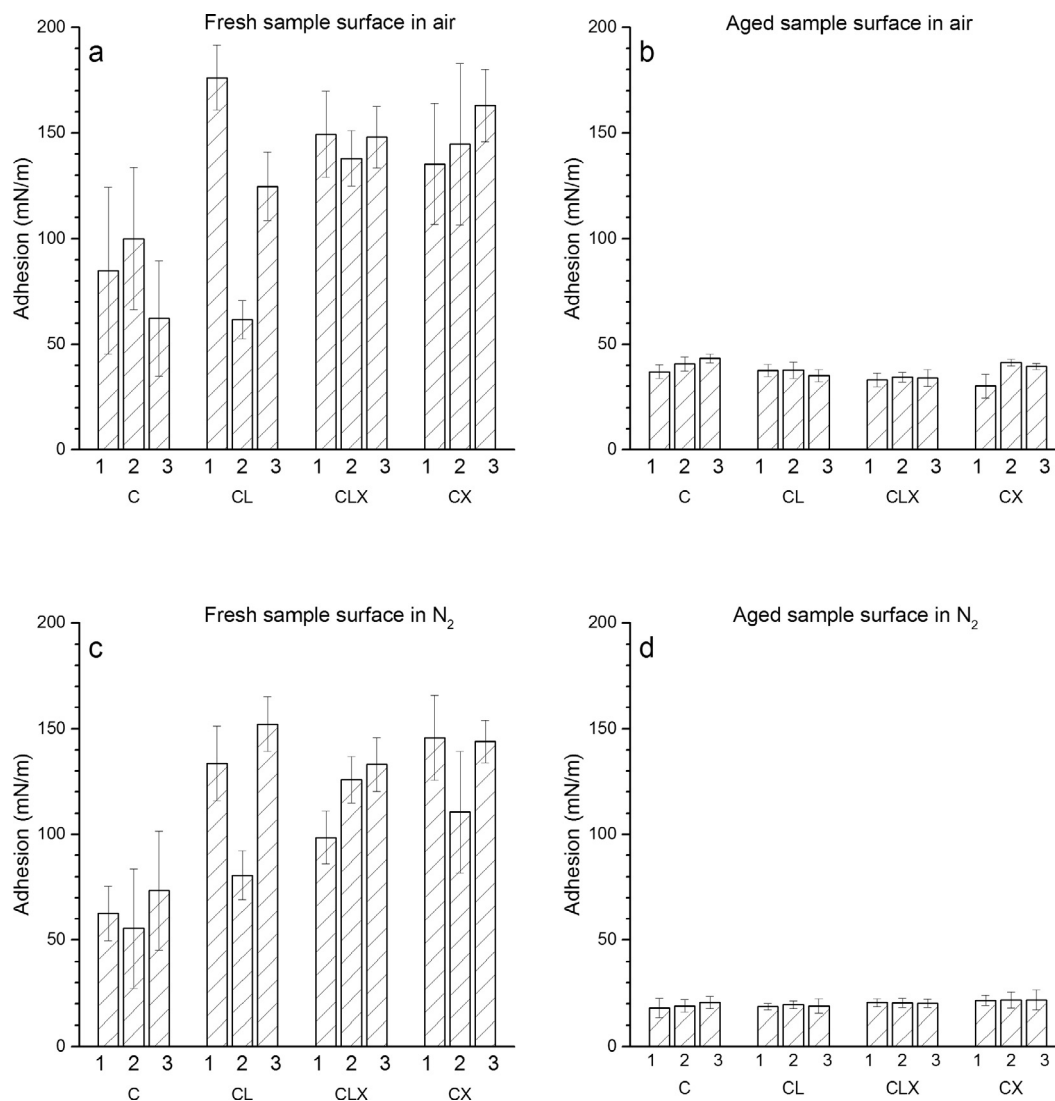
Fig. 4. Normalized pull-off forces (adhesion) measured on fresh and aged surfaces in various atmospheres: (a) fresh surface in air, (b) aged surface in air, (c) fresh surface in N_2, (d) aged surface in N_2. Each bar corresponds to the mean value of 100 measurements on a fibre cross section. Error bars represent the standard deviation.

slightly raise the overall adhesion properties of the CX fibres. Similarly, CL fibres still contain 4.35% xylan. Unfortunately, production of CX fibres containing no lignin at all and of CL fibres without xylan was not achieved. This makes conclusions on the impact of an individual component challenging, and we cannot exclude other parameters than polar and disperse interactions to be involved in the adhesion between the fibre cross section and the PLA microsphere.

The adhesion behaviour between two components is closely related to the applied pressure and to their surface energy [41,42], and different adhesion mechanisms can contribute to the final adhesion between two objects. With our experimental design, we can neglect two of them: mechanical interlocking (due to smooth surfaces) and inter-diffusion (due to short contact time and temperatures below the glass transition temperature of the respective materials). Hence, the adhesion we observe is either due to chemical bonding or interfacial energy or a combination of both. Therefore, we evaluated the surface energy as well as the acid and base dissociation constant of the regenerated lignocellulosic fibres through IGC. Elucidation of the surface energy could provide explanations for the differences in pull-off forces obtained with the colloidal probe technique. However, key differences should be highlighted: while measurements with colloidal probe
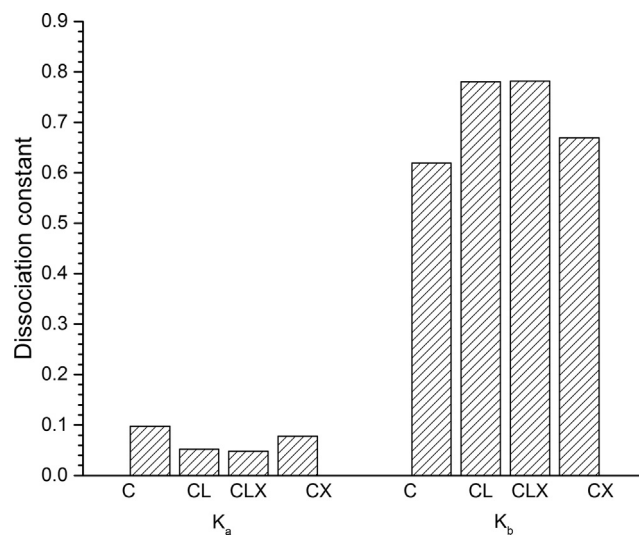

Fig. 5. Acid and base constants of the four fibre types as measured by IGC.

technique were performed on the fibre cross-sections, IGC only allows assessing the surface energy of the outer surface of the aged fibres. For this reason, no comparison between fresh and aged surfaces is possible with IGC. The IGC results are presented in Figs. 5 and 6. The acid and base dissociation constants (Fig. 5) suggest that the fibres are of basic character ($K_b > K_a$). Presence of lignin and/or xylan increases the base dissociation constant. In the case of hemicellulose (xylan), this can be related to its strong basicity and weak acidity [43,44]. However, besides the amount of each component in the fibre, other parameters such as crystallinity or homogeneity of the composition between bulk and surface come into play. This makes general statements about the specific contribution of each individual component difficult, as studies on various natural fibres have shown [45].

All fibres show total surface energy (γ_t) values below 50 mJ/m^2 (Fig. 6a), which is in accordance with previously published data on lignocellulosic natural fibres [46–48]. The values measured for the PLA microspheres are also in accordance with literature [49]: our measurements resulted in an acid-base component of 8.5 mJ/m^2 and a disperse component of 39.9 mJ/m^2. Moreover, the total surface energy is lower for the fibres containing lignin and/or xylan. For fibres containing both lignin and xylan (CLX), the total surface energy is lowest. This pattern also appears in the case of the acid-base component (γ_{AB}, also called polar component). Concerning the disperse part of the surface energy (γ_D), it is only affected when both lignin and xylan are present in the fibre. These results fit well with other values obtained using tensiometry [50], even though the share of polar and disperse contribution is somewhat different:
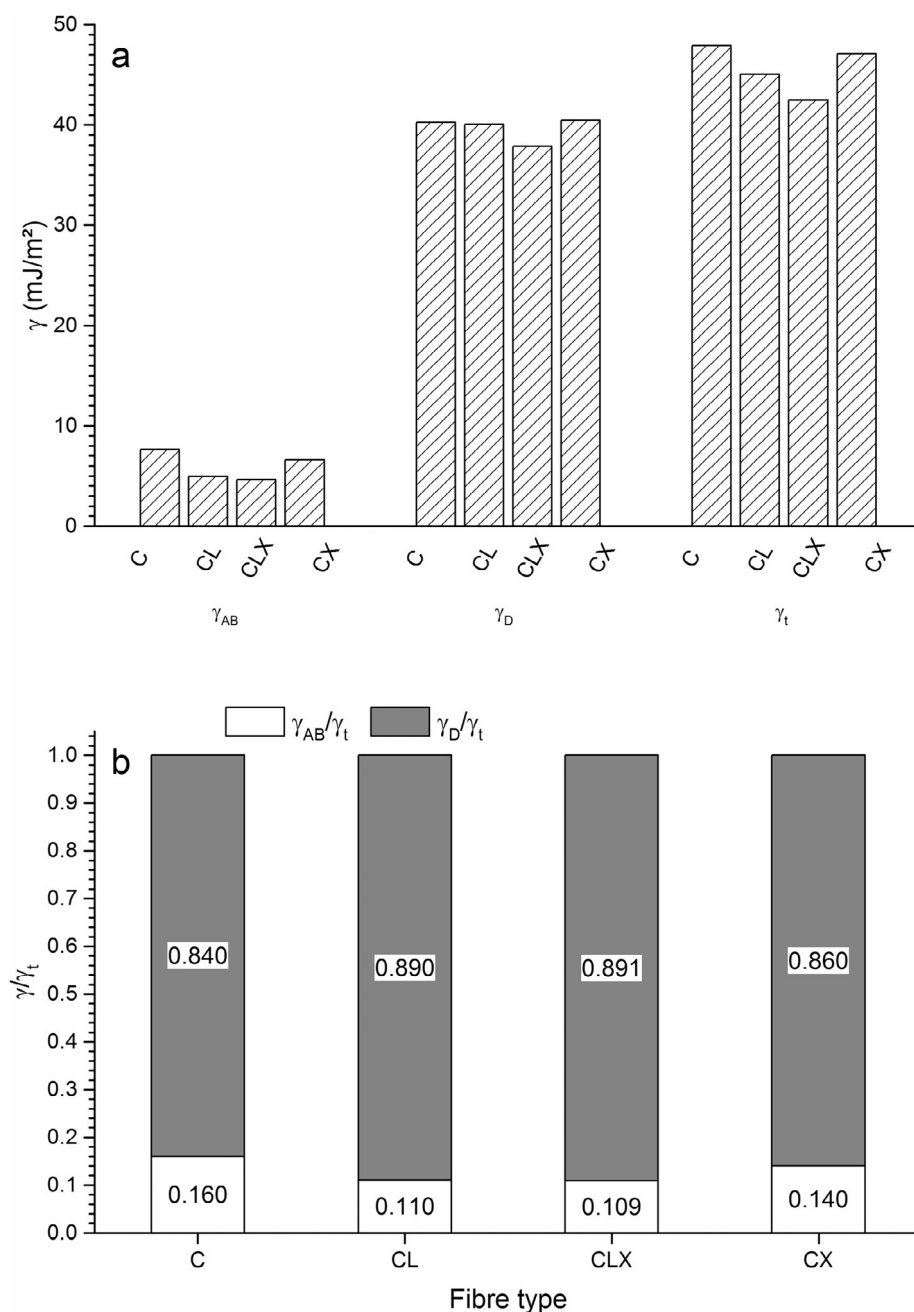

Fig. 6. Surface energies as obtained by IGC (a) and share of polar and dispersive components in the total surface energy (b) for all fibre types.

while the results obtained with IGC indicate that the major part of the total surface energy is made out by the disperse component, the distribution was found to be more balanced (50% disperse part, 50% polar part) when using tensiometry. This could be related to the bias introduced by the swelling of the fibres during the tensiometric measurement, as pointed out by the authors themselves [50]. As the fibres do not swell during the IGC measurements, the results presented in this study should not be biased. Fig. 6b shows that, for both CL and CLX, acid-base surface energy amounts to 11% of the total surface energy. This percentage is higher in CX and C, with values of 14% and 16%, respectively. This suggests that the polarity of the fibres decreases when lignin is added, while the effect of xylan is more limited – it slightly impacts the absolute surface energy values but not the relative share of the polar and dispersive components.

Fig. 7 shows the individual adhesion force values obtained on selected samples with aged surface. In Fig. 4, only mean values and standard deviations were represented, no systematic differences could be found among the samples. However, when looking at all the values obtained during a measurement (i.e. plotted over time), a specific pattern appears. Adhesion on neat cellulose (C sample) linearly increases by about 10–15 mN/m in the course of the measurement, while the adhesion stays constant on the other samples. This is valid in air as well as in dry N_2 atmosphere. The two other fibre types (CL and CX) behaved similarly as CLX, show-

ing rather constant adhesion values along the measurements (compare supplementary information S2). On fresh surfaces, the existence of similar trends is possible, but the higher standard deviation within a measurement series does not allow drawing conclusions.

As evident from Fig. 4, the adhesion force is lower on aged samples than on fresh ones. Linear increase in adhesion force with the measurement number (i.e. with time) as shown in Fig. 7 seems to contradict this finding. This suggests that the affinity of the fibres towards PLA is only increasing during the measurement itself. For example, residual humidity on the microsphere or on the fibre surface may cause this unintended drift in air, yet does not explain the increase in nitrogen atmosphere.

For the neat cellulose sample, being the most hydrophilic one, the observed trends may be related to capillary water. Indeed, as already stated before, ambient humidity can cause the formation of a thin water layer between the sample surface and the PLA microsphere. Hydrophilic regenerated fibres (as it is the case for C fibres) may enhance this effect as the water could slowly accumulate on the sample surface. The thickness of the humid layer could therefore increase during the measurement, thereby affecting capillary forces and adhesion. However, it seems quite paradoxical that this trend also occurs in dry N_2 atmosphere where no capillary forces should be involved. One hypothetical explanation would be that water is trapped in the C fibres and is "squeezed
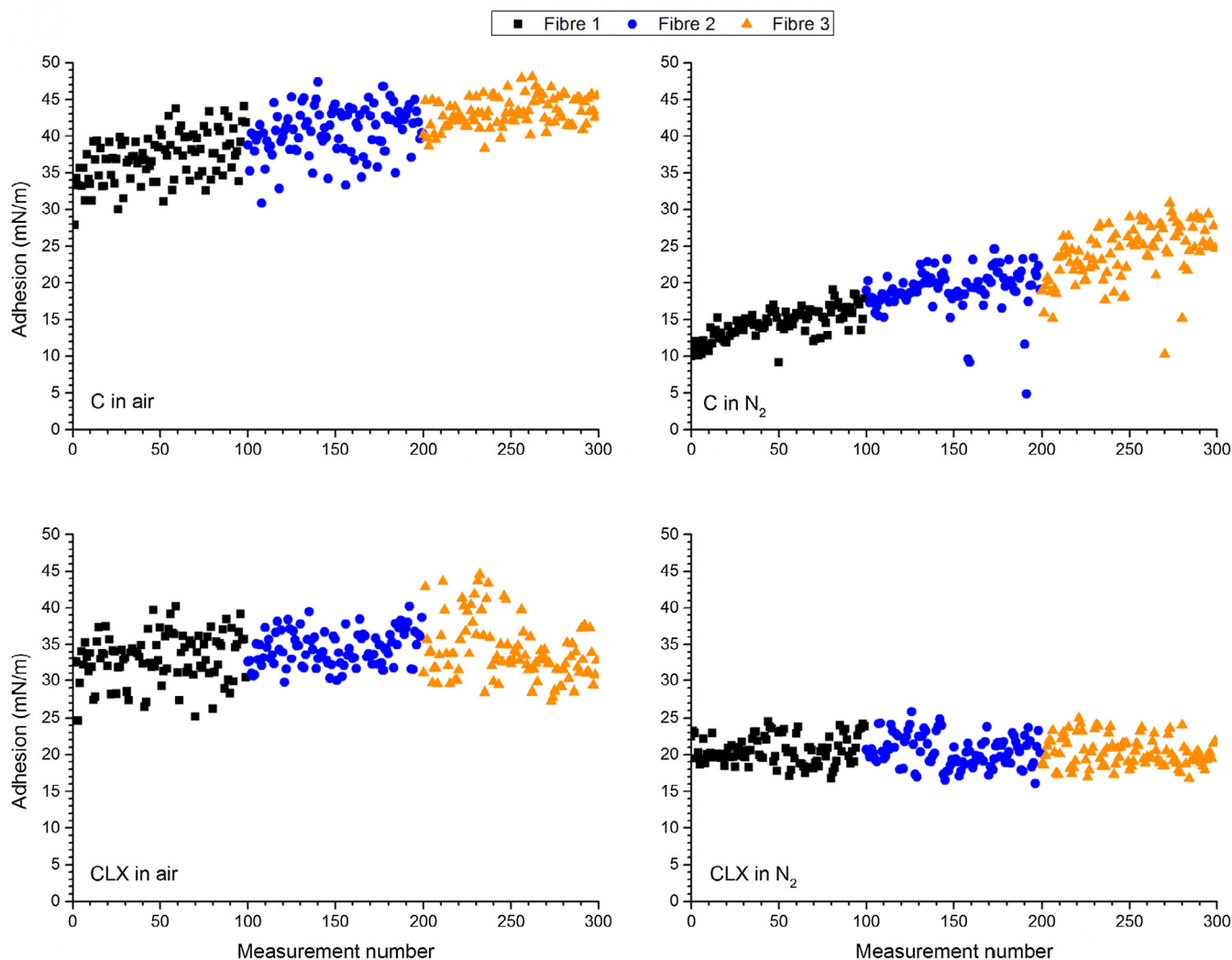

Fig. 7. Individual adhesion force values obtained on aged cross-sections of C and CLX fibres in air and N_2.

out" when the PLA microsphere presses on the fibre cross-section. This would cause very local water accumulations to be present on the fibre surface even in a nitrogen atmosphere. In the other samples (CL, CLX and CX), the presence of rather hydrophobic lignin could stop this phenomenon from happening. However, further research is needed to verify the validity of this assumption. Moreover, other factors such as the degree of orientation or the crystallinity may play a role in the interaction between the substrate and the PLA spheres. In xylan-containing nanofibrillated cellulose, these properties have been shown to influence the water adsorption and desorption as measured by Dynamic Vapor Sorption (DVS) [51].

4. Conclusions

Incompatibility between phases of different polarity is a crucial issue in the field of polymer research. In the case of natural fibre reinforced composites, the influence of the chemical components present in the fibres has been investigated in the past [4–6]. Model compounds can be used to overcome the inherent variability in surface properties of natural fibres [10]. From the experimental point of view, several methods can be used for the assessment of interfacial interactions between two materials [8–13]. In the present work, the adhesion behaviour of regenerated lignocellulosic fibre cross-sections with regard to PLA was investigated with the colloidal probe technique for the first time. As expected, aged sample surfaces showed much less adhesion than fresh ones. The distribution of adhesion values was also much broader on the fresh samples. Furthermore, elimination of capillary forces achieved by switching to a dry atmosphere resulted in a lower adhesion than what was detected in ambient air. When it comes to comparing the different fibre types used in this study, no difference in the adhesion could be detected on aged surfaces, suggesting the occurrence of oxidation reactions. However, when the adhesion was measured immediately after cutting a fresh surface, the fibres containing only cellulose clearly showed lower adhesion towards PLA, both in ambient air and in dry N_2 atmosphere. The presence of lignin and/or xylan led to an increase in the adhesion because of its comparably lower polarity. The influence of capillary forces could not be totally removed, even though it played a much less important role in N_2 compared to air. All in all, the presence of lignin and hemicellulose in freshly cut regenerated lignocellulosic fibres resulted in larger adhesion, indicating a more favourable interaction with the PLA microsphere. Lignin had an influence on the share of polar and disperse surface energy components, while xylan did only impact the absolute values. As adhesion and surface energy are major parameters to evaluate compatibility between different phases, lignin and xylan could be applied as coupling agents in the future.

5. Author contributions

J.C. planned the experiments, performed the colloidal probe measurements, analysed the data and wrote the preliminary manuscript. T.P. introduced J.C. to the colloidal probe technique and supervised his work during his research stay at KTH. H.S., S.A and T.N. produced and characterized the regenerated lignocellulosic fibres. A.M. performed the IGC measurements and processed the IGC data. J.K. supervised the work. The manuscript was written through contributions of all authors. All authors read the final version of the manuscript and approved it.

6. Notes

The authors declare no competing financial interest.

Appendix A. Supplementary material

Supplementary data associated with this article can be found, in the online version, at https://doi.org/10.1016/j.jcis.2018.08.032.

References

[1] S.V. Joshi, L.T. Drzal, A.K. Mohanty, S. Arora, Are natural fiber composites environmentally superior to glass fiber reinforced composites?, Compos Part A Appl. Sci. Manuf. 35 (2004) 371–376, https://doi.org/10.1016/j.compositesa.2003.09.016.
[2] D. Maldas, B. Kokta, Influence of maleic anhydride as a coupling agent on the performance of wood fiber-polystyrene composites, Polym. Eng. Sci. 31 (1991) 1351–1357. http://onlinelibrary.wiley.com/doi/10.1002/pen.760311810/abstract.
[3] A.V. Singhal, K. Debnath, I. Singh, B.S.S. Daniel, Critical parameters affecting mechanical behavior of natural fiber reinforced plastics, J. Nat. Fibers 13 (2016) 640–650, https://doi.org/10.1080/15440478.2015.1102788.
[4] W. Thielemans, R.P. Wool, Butyrated kraft lignin as compatibilizing agent for natural fiber reinforced thermoset composites, Compos. Part A Appl. Sci. Manuf. 35 (2004) 327–338, https://doi.org/10.1016/j.compositesa.2003.09.011.
[5] G. Xu, G. Yan, J. Zhang, Lignin as coupling agent in EPDM rubber: thermal and mechanical properties, Polym. Bull. 72 (2015) 2389–2398, https://doi.org/10.1007/s00289-015-1411-7.
[6] A. Winter, L. Andorfer, S. Herzele, T. Zimmermann, B. Saake, M. Edler, et al., Reduced polarity and improved dispersion of microfibrillated cellulose in poly (lactic-acid) provided by residual lignin and hemicellulose, J. Mater. Sci. 52 (2017) 60–72, https://doi.org/10.1007/s10853-016-0439-x.
[7] G. Binnig, C.F. Quate, Atomic force microscope, Phys. Rev. Lett. 56 (1986) 930–933, https://doi.org/10.1103/PhysRevLett. 56.930.
[8] T. Pettersson, S.A. Pendergraph, S. Utsel, A. Marais, E. Gustafsson, L. Wågberg, Robust and tailored wet adhesion in biopolymer thin films, Biomacromolecules 15 (2014) 4420–4428, https://doi.org/10.1021/bm501202s.
[9] A. Naderi, J. Iruthayaraj, T. Pettersson, R. Makuška, P.M. Claesson, Effect of polymer architecture on the adsorption properties of a nonionic polymer, Langmuir 24 (2008) 6676–6682, https://doi.org/10.1021/la800089v.
[10] E. Gustafsson, E. Johansson, L. Wågberg, T. Pettersson, Direct adhesive measurements between wood biopolymer model surfaces, Biomacromolecules 13 (2012) 3046–3053, https://doi.org/10.1021/bm300762e.
[11] W.A. Ducker, T.J. Senden, R.M. Pashley, Direct measurement of colloidal forces using an atomic force microscope, Nature 353 (1991) 239–241, https://doi.org/10.1038/353239a0.
[12] H.J. Butt, Measuring electrostatic, van der Waals, and hydration forces in electrolyte solutions with an atomic force microscope, Biophys. J. 60 (1991) 1438–1444, https://doi.org/10.1016/S0006-3495(91)82180-4.
[13] M. Kappl, H.J. Butt, The colloidal probe technique and its application to adhesion force measurements, Part. Part. Syst. Charact. 19 (2002) 129–143. Doi 10.1002/1521-4117(200207)19:3<129::Aid-Ppsc129>3.0.Co;2-G.
[14] B.V. Derjaguin, Untersuchungen uber die Reibung und Adhesion, IV. Theorie des Anhaften kleiner Teilchen, Koll. Ztschr. 69 (1934) 155–164.
[15] E.J.W. Verwey, E.T.G. Overbeek, Theory of the stability of lyophobic colloids, J. Colloid Sci. 10 (1955) 224–225.
[16] M. Holmberg, R. Wigren, R. Erlandsson, P.M. Claesson, Interactions between cellulose and colloidal silica in the presence of polyelectrolytes, Colloids Surfaces A Physicochem. Eng. Asp. 129–130 (1997) 175–183, https://doi.org/10.1016/S0927-7757(97)00036-8.
[17] I.L. Radtchenko, G. Papastavrou, M. Borkovec, Direct force measurements between cellulose surfaces and colloidal silica particles, Biomacromolecules 6 (2005) 3057–3066, https://doi.org/10.1021/bm050371d.
[18] M. Rutland, A. Carambassis, G. Willing, R. Neuman, Surface force measurements between cellulose surfaces using scanning probe microscopy, Colloids Surfaces A Physicochem. Eng. Asp. 123–124 (1997) 369–374, https://doi.org/10.1016/S0927-7757(96)03790-9.
[19] C. Carrick, S.A. Pendergraph, L. Wågberg, Nanometer smooth, macroscopic spherical cellulose probes for contact adhesion measurements, ACS Appl. Mater. Interfaces. 6 (2014) 20928–20935, https://doi.org/10.1021/am505673u.
[20] S.M. Notley, M. Norgren, Measurement of interaction forces between lignin and cellulose as a function of aqueous electrolyte solution conditions, Langmuir 22 (2006) 11199–11204, https://doi.org/10.1021/la0618566.

[21] G. Raj, E. Balnois, M.A. Helias, C. Baley, Y. Grohens, Measuring adhesion forces between model polysaccharide films and PLA bead to mimic molecular interactions in flax/PLA biocomposite, J. Mater. Sci. 47 (2012) 2175–2181, https://doi.org/10.1007/s10853-011-6020-8.

[22] S. Utsel, A. Carlmark, T. Pettersson, M. Bergström, E.E. Malmström, L. Wågberg, Synthesis, adsorption and adhesive properties of a cationic amphiphilic block copolymer for use as compatibilizer in composites, Eur. Polym. J. 48 (2012) 1195–1204, https://doi.org/10.1016/j.eurpolymj.2012.05.004.

[23] H. Sixta, A. Michud, L. Hauru, S. Asaadi, Y. Ma, A.W.T. King, et al., Ioncell-F: A High-strength regenerated cellulose fibre, Nord. Pulp Pap. Res. J. 30 (2015) 43–57, https://doi.org/10.3183/NPPRJ-2015-30-01-p043-057.

[24] A. Sluiter, B. Hames, R. Ruiz, C. Scarlata, J. Sluiter, D. Templeton, et al., NREL/TP-510-42618 analytical procedure - Determination of structural carbohydrates and lignin, Biomass (2012). doi:NREL/TP-510-42618.

[25] P.B. O'Donnell, J.W. McGinity, Preparation of microspheres by the solvent evaporation technique, Adv. Drug Deliv. Rev. 28 (1997) 25–42, https://doi.org/10.1016/S0169-409X(97)00049-5.

[26] J.E. Sader, J.W.M. Chon, P. Mulvaney, Calibration of rectangular atomic force microscope cantilevers, Rev. Sci. Instrum. 70 (1999) 3967–3969, https://doi.org/10.1063/1.1150021.

[27] E. Thormann, T. Pettersson, P.M. Claesson, How to measure forces with atomic force microscopy without significant influence from nonlinear optical lever sensitivity, Rev. Sci. Instrum. 80 (2009), https://doi.org/10.1063/1.3194048.

[28] T.J. Senden, Force microscopy and surface interactions, Curr. Opin. Colloid Interface Sci. 6 (2001) 95–101.

[29] J. Colson, L. Andorfer, T.E. Nypelö, B. Lütkemeier, F. Stöckel, J. Konnerth, Comparison of silicon and OH-modified AFM tips for adhesion force analysis on functionalised surfaces and natural polymers, Colloids Surfaces A Physicochem. Eng. Asp. 529 (2017) 363–372, https://doi.org/10.1016/j.colsurfa.2017.06.017.

[30] T.E. Nypelö, C. Laine, J. Colson, U. Henniges, T. Tammelin, Submicron hierarchy of cellulose nanofibril films with etherified hemicelluloses, Carbohydr. Polym. 177 (2017) 126–134, https://doi.org/10.1016/j.carbpol.2017.08.086.

[31] S. Frybort, M. Obersriebnig, U. Müller, W. Gindl-Altmutter, J. Konnerth, Variability in surface polarity of wood by means of AFM adhesion force mapping, Colloids Surfaces A Physicochem. Eng. Asp. 457 (2014) 82–87, https://doi.org/10.1016/j.colsurfa.2014.05.055.

[32] Y. Ma, S. Asaadi, L.S. Johansson, P. Ahvenainen, M. Reza, M. Alekhina, et al., High-strength composite fibers from cellulose-lignin blends regenerated from ionic liquid solution, ChemSusChem. 8 (2015) 4030–4039, https://doi.org/10.1002/cssc.201501094.

[33] J. Sjöberg, A. Potthast, T. Rosenau, P. Kosma, H. Sixta, Cross-sectional analysis of the polysaccharide composition in cellulosic fiber materials by enzymatic peeling/high-performance capillary zone electrophoresis, Biomacromolecules 6 (2005) 3146–3151, https://doi.org/10.1021/bm050471j.

[34] M. Gindl, A. Reiterer, G. Sinn, S.E. Stanzl-Tschegg, Effects of surface ageing on wettability, surface chemistry, and adhesion of wood, Holz Als Roh - Und Werkst. 62 (2004) 273–280, https://doi.org/10.1007/s00107-004-0471-4.

[35] R.M. Nussbaum, M. Sterley, The effect of wood extractive content on glue adhesion and surface wettability of wood, Wood Fiber Sci. 34 (2002) 57–71.

[36] M.E.P. Wålinder, Study of Lewis acid-base properties of wood by contact angle analysis, Holzforschung. 56 (2002) 363–371, https://doi.org/10.1515/HF.2002.058.

[37] K.L. Kato, R.E. Cameron, Structure-property relationships in thermally aged cellulose fibers and paper, J. Appl. Polym. Sci. 74 (1999) 1465–1477, https://doi.org/10.1002/(SICI)1097-4628(19991107)74:6<1465::AID-APP20>3.0.CO;2-3.

[38] D.L. Sedin, K.L. Rowlen, Adhesion forces measured by atomic force microscopy in humid air, Anal. Chem. 72 (2000) 2183–2189, https://doi.org/10.1021/ac991198c.

[39] R. Jones, H.M. Pollock, J.A.S. Cleaver, C.S. Hodgest, Adhesion forces between glass and silicon surfaces in air studied by AFM : effects of relative humidity, particle size, roughness, and surface treatment, Langmuir 18 (2002) 8045–8055.

[40] E.K. Gamstedt, R. Sandell, F. Berthold, T. Pettersson, N. Nordgren, Characterization of interfacial stress transfer ability of particulate cellulose composite materials, Mech. Mater. 43 (2011) 693–704, https://doi.org/10.1016/j.mechmat.2011.06.015.

[41] K. Kendall, The adhesion and surface energy of elastic solids, J. Phys. D Appl. Phys. 4 (1971) 1186–1195. http://iopscience.iop.org/0022-3727/4/8/320.

[42] K.L. Johnson, K. Kendall, A.D. Roberts, Surface energy and the contact of elastic solids, Proc. Roy. Soc. A Math. Phys. Eng. Sci. 324 (1971) 301–313, https://doi.org/10.1098/rspa.1971.0141.

[43] N. Cordeiro, M. Ornelas, A. Ashori, S. Sheshmani, H. Norouzi, Investigation on the surface properties of chemically modified natural fibers using inverse gas chromatography, Carbohydr. Polym. 87 (2012) 2367–2375, https://doi.org/10.1016/j.carbpol.2011.11.001.

[44] A. Ashori, M. Ornelas, S. Sheshmani, N. Cordeiro, Influence of mild alkaline treatment on the cellulosic surfaces active sites, Carbohydr. Polym. 88 (2012) 1293–1298, https://doi.org/10.1016/j.carbpol.2012.02.008.

[45] N. Cordeiro, C. Gouveia, A.G.O. Moraes, S.C. Amico, Natural fibers characterization by inverse gas chromatography, Carbohydr. Polym. 84 (2011) 110–117, https://doi.org/10.1016/j.carbpol.2010.11.008.

[46] J.A.F. Gamelas, The surface properties of cellulose and lignocellulosic materials assessed by inverse gas chromatography: A review, Cellulose 20 (2013) 2675–2693, https://doi.org/10.1007/s10570-013-0066-5.

[47] A. Legras, A. Kondor, M. Alcock, M.T. Heitzmann, R.W. Truss, Inverse gas chromatography for natural fibre characterisation: dispersive and acid-base distribution profiles of the surface energy, Cellulose 24 (2017) 4691–4700, https://doi.org/10.1007/s10570-017-1443-2.

[48] R.H. Mills, D.J. Gardner, R. Wimmer, Inverse gas chromatography for determining the dispersive surface free energy and acid-base interactions of sheet molding compound-Part II 14 ligno-cellulosic fiber types for possible composite reinforcement, J. Appl. Polym. Sci. 110 (2008) 3880–3888, https://doi.org/10.1002/app.

[49] D. Cava, R. Gavara, J.M. Lagarón, A. Voelkel, Surface characterization of poly (lactic acid) and polycaprolactone by inverse gas chromatography, J. Chromatogr. A. 1148 (2007) 86–91, https://doi.org/10.1016/j.chroma.2007.02.110.

[50] T.E. Nypelö, S. Asaadi, G. Kneidinger, H. Sixta, J. Konnerth, Dry-jet wet-spun wood-biopolymer macrofibers with tunable surface energy and strength, Cellulose (2018), https://doi.org/10.1007/s10570-018-1902-4.

[51] T.M. Tenhunen, M.S. Peresin, P.A. Penttilä, J. Pere, R. Serimaa, T. Tammelin, Significance of xylan on the stability and water interactions of cellulosic nanofibrils, React. Funct. Polym. 85 (2014) 157–166, https://doi.org/10.1016/j.reactfunctpolym.2014.08.011.